Published in final edited form as:
Neuroradiology. 2013 February ; 55(2): 233–243. doi:10.1007/s00234-012-1122-9.

Whole-brain voxel-based analysis of diffusion tensor MRI parameters in patients with primary open angle glaucoma and correlation with clinical glaucoma stage

Hui Dai,
Department of Radiology, The First Affiliated Hospital of Soochow University, Shizi Street 188#, Suzhou, Jiangsu 215006, People's Republic of China

Dazhi Yin,
Key Laboratory of Brain Functional Genomics, Ministry of Education, Shanghai Key Laboratory of Brain Functional Genomics and Shanghai Key Laboratory of Magnetic Resonance, East China Normal University, Zhongshan North Road 3663#, Shanghai 200062, People's Republic of China

Chunhong Hu,
Department of Radiology, The First Affiliated Hospital of Soochow University, Shizi Street 188#, Suzhou, Jiangsu 215006, People's Republic of China

John N. Morelli,
Scott and White Memorial Hospital, Texas A&M Health Sciences Center, Temple, TX 76504, USA

Su Hu,
Department of Radiology, The First Affiliated Hospital of Soochow University, Shizi Street 188#, Suzhou, Jiangsu 215006, People's Republic of China

Xu Yan, and
Key Laboratory of Brain Functional Genomics, Ministry of Education, Shanghai Key Laboratory of Brain Functional Genomics and Shanghai Key Laboratory of Magnetic Resonance, East China Normal University, Zhongshan North Road 3663#, Shanghai 200062, People's Republic of China

Dongrong Xu
MRI Unit, Columbia University Dept. of Psychiatry, New York State Psychiatric Institute, 1051 Riverside Drive, NYSPI, Unit 74, New York, NY 10032, USA

Dongrong Xu: xud@childpsych.columbia.edu

Abstract

Introduction—Glaucoma is the second leading cause of blindness worldwide. The purpose of this study is to identify areas of neurodegeneration in glaucoma utilizing 3 T magnetic resonance (MR) diffusion tensor imaging (DTI) parameters with whole-brain voxel-based analysis (VBA) and determine whether these parameters correlate with disease severity.

Methods—Twenty-five glaucoma patients and 25 age-matched healthy volunteers were prospectively examined. Clinical glaucoma severity was assessed utilizing static threshold visual field parameters. All subjects underwent 3 T MRI utilizing a DTI sequence (repetition time/echo time 13,000/68.9 ms, maximal *b* value 800 s/mm^2 along 30 directions) and an anatomic sequence

Correspondence to: Dongrong Xu, xud@childpsych.columbia.edu.

Conflict of interest We declare that we have no conflict of interest.

to provide structural information. All data sets were processed by VBA. Brain fractional anisotropy, mean diffusivity (MD), radial diffusivity (RD), and axial diffusivity (AD) were compared in the two groups. Correlation between DTI parameters and glaucoma stage were determined.

Results—The bilateral optic radiations and chiasma of glaucoma patients demonstrated statistically significantly lower fractional anisotropy ($p<0.05$). Optic radiation RD was similarly decreased in glaucoma patients ($p<0.05$). There were no statistically significant differences noted in MD or AD between the two groups ($p>0.05$). Optic chiasm fractional anisotropy values were negatively correlated with glaucoma stage ($r=-0.53$, $p<0.05$) and optic radiation RD values positively correlated (left $r=0.45$, $p<0.05$; right = 0.38, $p=0.06$).

Conclusion—DTI parameters fractional anisotropy and RD are altered in the optic chiasm and radiations of glaucoma patients. As fractional anisotropy and RD also correlate with glaucoma stage, these values could serve as potential non-invasive markers of disease severity.

Keywords

Primary open-angle glaucoma; Magnetic resonance imaging; Diffusion tensor imaging; Voxel-based analysis

Introduction

Primary open angle glaucoma (POAG) is an irreversible optic neuropathy characterized by progressive loss of retinal ganglion cells and their axons. Patients with glaucoma exhibit abnormal optic discs and visual field losses. The etiology of POAG has not yet been completely elucidated. Intraocular pressure (IOP) elevation is, thus far, the only proven and treatable risk factor [1]. However, even when elevated IOPs are treated effectively, glaucoma may worsen [2], suggesting other independent factors associated with progression [3]. Recent studies have demonstrated an association between high IOPs in glaucoma and structural neurodegenerative changes in the retina, lateral geniculate nucleus, and visual cortex [4–6]. Pathologically, dendritic damage, cell body shrinkage, and death are ultimately manifest as a progressive loss of cell population leading clinically to vision loss [7–9]. Functional MRI [10, 11] and magnetic transfer imaging [10] have likewise been utilized to evaluate central nervous system (CNS) changes in POAG.

Diffusion tensor imaging (DTI) is a structural MRI technique depicting water diffusion directionality [12] and has proven useful in studying white matter disease and cranial nerve disorders [13–15]. Both measures of radial diffusivity (RD) and axial diffusivity (AD) can be obtained, and experimental data in animals suggests abnormalities in RD and AD correlate with myelin and axonal damage, respectively [16, 17]. For example, in Alzheimer's disease, increased RD and loss of AD suggest both the presence of axonal loss in combination with Wallerian degeneration [18, 19], and increased RD has also been demonstrated in patients with optic neuritis [20]. Recently, DTI has been applied to glaucoma using various postprocessing techniques, such as region of interest segmentations [21, 22]. An initial result found foci of increased RD along the optic radiations [23], and another study correlated the extent of RD abnormalities to glaucoma stage [24]. However, these studies examined only the optic radiations. An additional prior study used tract-based spatial statistics (TBSS) to study brain DTI in glaucoma patients[25]; however, AD and RD were not assessed and no study to date has evaluated these parameters in a full-brain DTI analysis.

The purpose of this study is to detect which DTI parameters, if any, will be altered in POAG and where these alterations will occur. This is tested utilizing 3 T MR DTI in a whole-brain

voxel-based morphometry analysis. It is also determined whether these parameters correlate with POAG severity.

Methods

Subjects

This study was approved by the local institutional review board and is in compliance with the Declaration of Helsinki. From March to August 2010, two participant groups were included in this prospective study: a group of glaucoma patients and a control group age- and sex-matched normal volunteers. Informed consent was obtained from all participants. The glaucoma group consisted of 25 consecutive patients with ages ranging from 21 to 54 years (34.5± 10.5 years) with a diagnosis of POAG. Exclusion criteria were patients (1) under 18 years of age; (2) with secondary glaucoma, closed angle, pigment dispersion, or pseudoexfoliation; (3) with other ophthalmologic disorders; (4) with a history of cardiovascular disease or diabetes; and (4) with a history of any CNS disorder including small vessel ischemic white matter disease found on the initial MRI. The glaucoma diagnosis was made clinically through assessment of the open anterior chamber angle, identification of visual field defects typical of glaucoma, optic disc cupping, or identification of an IOP of 21 mmHg or greater. The 25 healthy volunteers' ages ranged from 21 to 55 years (35.3±11.2 years). All volunteers underwent ophthalmologic examination to exclude individuals with myopia or hyperopia greater than 200°, amblyopia, glaucoma, or other oculopathy. There were no statistically significant differences between the mean ages of the patient and control groups (p>0.05). Both groups contained 19 men and six women.

Hodapp-Anderson-Parrish system

The Hodapp–Anderson–Parrish (HAP) system [11] was utilized to stage the eyes of all glaucoma patients (stages 0–5) within 1 month of the MR examination. Stage 0 glaucoma was defined as increased IOP without evidence of visual field defects and with a mean deviation score (MDS) higher than 0 dB. Stage 1 (early) was defined as a MDS from −0.01 to −6.00 dB, stage 2 (moderate) from −6.01 to −12.00 dB, and stage 3 (advanced) from −12.01 to −20.00 dB. Stage 4 (severe) was defined as a MDS less than −20.01 dB. For patients designated clinically as stage 5, static threshold perimetry was not performed. The cup to disk ratio (C/D), retinal nerve fiber layers (RNFL), IOP, and MDS values of both eyes for each patient are provided in Table 1. A summation of the clinical stage of each eye was utilized to assess total severity for each patient.

MR examination

All subjects underwent 3 T MR imaging (Signa HDxt, GE Healthcare, Milwaukee, WI, USA). An eight-channel phased-array head coil was utilized for signal reception. Subjects were scanned head first and supine. Head position was fixed with foam cushions on both sides. The following sequences were acquired: an axial 3D Brain Volume Imaging (BRAVO) sequence (repetition time/echo time/inversion time 6.8/3.5/380 ms, slice thickness 1.0 mm without inter-slice gaps, matrix 256×256, field of view 256 mm^2, one scan average, bandwidth 42 Hz, flip angle 15°, scan time 2:43 min:s) and an isotropic DTI sequence (repetition time/echo time 13,000/68.9 ms, slice thickness 2 mm without interslice gaps, matrix 128×128, field of view 256 mm^2, two scan averages, b=800 s/mm^2, number of directions 30, scan time 13:39 min:s). During the scan, subjects were told to lie still with their eyes stationary to reduce artifacts from motion. The 3D Brain Volume Imaging series for acquisition of T1-weighted images was similar to the more conventionally used three-dimensional fast spoiled gradient recall echo sequence. Although the spatial resolution of the 3D Brain Volume Imaging sequence is less than that typically obtained with three-dimensional fast-spoiled gradient recall echo, the resolution was adequate to provide precise

localization of anatomical structures corresponding to those identified via DTI and the acquisition time shorter.

Data processing

DTI preprocessing was performed using FMRIB's free software FSL (Oxford Centre for Functional MRI of the Brain, UK) as follows: (1) all diffusion-weighted images were checked visually by two experienced radiologists for apparent artifacts; (2) for each participant, diffusion-weighted images were registered to corresponding b=0 images with an offline transformation to correct eddy-current distortion; (3) binary brain masks of each participant from respective b=0 images were obtained using the Brain Extract Tools (BET) functionality for brain extraction; and (4) using FMRIB's diffusion tools (FDT), the diffusion tensor of each voxel within the brain mask was calculated by a linear least-square fitting algorithm. After diagonalization of the diffusion tensor, three diffusion tensor eigenvalues ($\lambda_1>\lambda_2>\lambda_3$) were obtained. A series of diffusion-related parameter maps involving fractional anisotropy (FA), mean diffusivity (MD), AD, and RD were derived from the following equations:

$$\mathrm{FA}=\frac{\sqrt{(\lambda_1-\lambda_2)^2+(\lambda_2-\lambda_3)^2+(\lambda_3-\lambda_1)^2}}{\sqrt{2}\sqrt{\lambda_1{}^2+\lambda_2{}^2+\lambda_3{}^2}}$$

$$\mathrm{MD}=\frac{\lambda_1+\lambda_2+\lambda_3}{3}$$

$$\mathrm{AD}=\lambda_1$$

$$\mathrm{RD}=\frac{(\lambda_2+\lambda_3)}{2}$$

FA reflects the extent of directionality in the water molecular motion; MD reflects the average magnitude of its motion; AD measures diffusivity of water molecules in the direction parallel to the principal direction of diffusion, and RD measures diffusivity perpendicular to the direction of principle diffusion.

Voxel-based analysis (VBA) of FA, MD, AD, and RD was performed with Statistical Parametric Mapping (SPM8, http://www.fil.ion.ucl.ac.uk/spm). Accurate image registration is critical to obtaining precise VBA. Moreover, some diffusion-related parameters may be affected by white matter degeneration caused by diseases such as glaucoma. In order to improve accuracy, VBA was implemented as follows: first, b=0 images of each healthy control were normalized to Montreal Neurological Institute space based on an EPI template and normalized b=0 images of all healthy controls were averaged. Next, the averaged b=0 images were spatially smoothed by using an isotropic Gaussian filter with a full width at half maximum of 6 mm. Thus, a new template of b=0 images was obtained in the Montreal Neurological Institute space. Subsequently, individual b=0 images of both patients and healthy controls were registered to the new template, and corresponding transformation matrixes were also obtained. Then, the FA, MD, AD, and RD maps of each participant were normalized to Montreal Neurological Institute space using their respective transformation

matrix and smoothed using an isotropic Gaussian filter with a full width at half maximum of 6 mm. Finally, a paired *t* test was performed for smoothed FA, MD, AD, and RD values obtained, respectively, between patients and healthy controls. The thresholds were set at $p<0.05$ (corrected for false discovery rate) with a minimum cluster size of 200 voxels.

Statistical analysis

After the paired *t* tests between patients and controls were performed, *t* value maps of FA, MD, AD, and RD were obtained. Masks of the given parameters of interest were abstracted from areas where differences between patients and volunteers were identified on the *t* value maps. In Montreal Neurological Institute (MNI) space, the mean FA, MD, AD, and RD values of the mask areas in each subject were calculated by placing the mask onto each participant's FA, MD, AD, and RD maps. Eventually, mean FA, MD, AD, and RD values for each subject in each area of statistically significant difference were obtained. Correlation between these values versus total glaucoma stages of patients were calculated utilizing the Spearman's nonparametric correlation test. As age-related cerebral volume loss could influence this correlation, an additional Spearman's correlation coefficient was computed to assess the relationship between patient age and the DTI parameters that exhibited a strong correlation clinical stage. Similar tests were performed to test the relationship of the aforementioned parameters to the mean RNFL of both eyes. The statistical analysis was performed with standard statistical software (SPSS version 13.0, SPSS). *P* values less than 0.05 were considered statistically significant.

Results

Mean FA of the optic chiasm and bilateral optic radiations in the POAG group was statistically significantly less than that of the control group (chiasm 0.16±0.02 versus 0.20±0.02, left optic radiation 0.40±0.03 versus 0.46±0.03, right optic radiation 0.38±0.04 versus 0.44±0.04, $p<10^{-3}$; Fig. 1, Table 2). Mean RD values of the bilateral optic radiations in glaucoma patients were statistically significantly greater than those of the control group (left optic radiation $0.68\pm0.04\times10^{-3}mm^2/s$ versus $0.61\pm0.03\times10^{-3}mm^2/s$, right optic radiation $0.71\pm 0.05\times10^{-3}mm^2/s$ versus $0.62\pm0.05\times10^{-3}mm^2/s$, $p<10^{-3}$; Fig. 2, Table 3). There were no statistically significant differences demonstrated in MD and AD between patients and controls ($p>0.05$), nor were any other differences in RD or FA found. Overall, the FA values of the optic chiasm were negatively correlated with the clinical stages of glaucoma patients ($r=-0.53$, $p<0.05$; Fig. 3), whereas the RD values of the left optic radiation were positively correlated with clinical stages ($r=0.45$, $p<0.05$; Fig. 4). RD values of the right optic radiation were also positively correlated with the clinical stage, although this correlation was just below the level of statistical significance ($r=0.38$, $p=0.06$; Fig. 5). Age was not statistically significantly correlated with optic radiation RD values nor with optic chiasm FA values (Figs. 3–5). The correlation coefficients between RNFL and the aforementioned DTI parameters are provided in Table 4. Only the correlation with optic chiasm FA was statistically significant.

Discussion

This study identifies DTI abnormalities in POAG patients in terms of mean, axial, and RD as well as functional anisotropy in a whole-brain analysis, correlating these changes with glaucoma stage and retinal thickness. DTI abnormalities in the glaucoma group were localized to the bilateral optic radiations and optic chiasma. Mean optic chiasm and radiation FA values were reduced, and optic radiation RD values increased. No statistically significant differences were detected for MD or AD. Optic chiasm FA values and optic radiation RD values correlated with glaucoma stage but not age. Optic chiasm FA values also correlated

with mean retinal nerve thickness. These findings are overall in agreement with those of smaller prior studies with several key differences that will be subsequently examined.

No previous study to date has comprehensively examined DTI parameters in whole-brain evaluations of glaucoma patients. VBA is a hypothesis-free, whole-brain, voxel-by-voxel method that compares imaging data between populations [26]. DTI VBA essentially searches the brain to find regions (voxels) that differ between groups without predetermining regions for hypothesis-driven evaluations. Thus, VBA successfully avoids selection biases of region of interest DTI postprocessing techniques. In a smaller study, Zikou et al. [25] used TBSS to study brain DTI in glaucoma patients; however, axial and RD were not assessed. Diffusion abnormalities were present not only within the optic chiasm and radiations but also in additional brain regions outside the visual system. In distinction, our study found all statistically significant FA decreases to be confined to the visual pathway. This discrepancy may relate to the relatively strict threshold we employed (i.e., cluster size of 200) or to the different statistical approaches (VBA in the present study versus TBSS in Zikou et al.). Likewise, the strict threshold utilized may have resulted in the apparent absence of glaucoma-related DTI changes within the optic tracts. Of note, t value maps of FA qualitatively demonstrated alterations extending into the proximal optic tracts, although the demarcation between the optic chiasm and proximal tracts is not precisely defined. The techniques employed in this study are also limited in their evaluation of the optic nerves, the DTI parameters of which, it would stand to reason, would be affected in POAG. Evaluation of the optic nerves by our DTI technique is challenging due to a number of factors, including their small size, long DTI acquisition times that may accentuate the affects of optic nerve motion, and bulk susceptibility artifacts related to adjacent air-filled paranasal sinuses. A rapid DTI sequence specifically designed for assessment of the optic nerves with an acquisition time under 10 min has been described and could be implemented in future studies to analyze the effects of POAG on the DTI parameters of these structures [27].

Myelin sheaths encasing axons are surmised to be the major restrictor of diffusion perpendicular to the axon, as their lipid bilayers have limited water permeability. Diffusivity longitudinal to the axons is not limited by such barriers, and axons consist of longitudinally oriented, cylindrical neurofibrils, interconnected by small microfilaments. These microstructures are related to the need for fast axonal transport [12]. Although controversial [28], several parameters have been derived from the diffusion tensor to describe different aspects of diffusion. Increased RD has been shown experimentally to reflect demyelination and decreased AD axonal damage [16, 17]. In our study, spectral components of the interpolated diffusion tensors were obtained using eigenvalue decomposition. From eigenvalues of the diffusion tensors, the relevant DTI parameters were calculated. The results of our study with respect to AD and RD are in agreement with a previous, smaller study by El-Rafei et al. focusing on DTI differences along the optic radiations [23]. In that study, areas of diminished RD were seen anterior within the right and posterior within the left optic radiation. No concentrated areas of AD value differences were found. This is in general agreement with our study that found both RD and FA but not AD values to be altered within the optic radiations. The alterations in DTI parameters in glaucoma may simply relate to transsynaptic degeneration; however, as increased RD correlates with demyelination in experimental work, this is another possibility worthy of consideration.

The extent of DTI changes in glaucoma patients has previously been shown to correlate with glaucoma severity. Garaci et al. [22] found a positive correlation between MD values and the clinical stage and a negative correlation between FA and the stage of glaucoma. In our study, optic chiasm and bilateral optic radiation FA values were statistically significantly less in glaucoma patients than in volunteers, consistent with the Garaci et al. study. More

recently, a smaller study demonstrated correlation between FA and RD values and glaucoma severity [24]. Our results are in agreement with these findings, supporting DTI parameters, RD and FA in particular, as noninvasive markers for glaucoma severity. The mechanism for why correlations between the right optic radiation RD and glaucoma stage were just below statistical significance is less clear and may relate to the asymmetry of disease observed or technical factors further elaborated upon below.

The present study is limited by the relatively small sample size. Strict exclusion criteria implemented to reduce the effects of concurrent neurological pathology resulted in a young glaucoma cohort compared to the general patient population. The concomitant effect of an aging brain (i.e., small vessel ischemic disease and atrophy) on DTI parameters was, thus, not examined. While prospective, this study does not include a longitudinal analysis of glaucoma patients. Nevertheless, in order to understand whether functional MRI techniques will be useful for assessment of glaucoma in the future, the nature and extent of CNS changes in the disease must first be thoroughly explored. This was the intent of the present work, and other promising avenues for further investigation are suggested. For example, the determination of DTI changes in patients undergoing therapy may prove useful in predicting clinical outcomes or monitoring therapeutic progress. Likewise, pretreatment assessment of CNS changes may be useful in establishing prognosis.

Other technical limitations of this study include the relatively long acquisition of the DTI sequence employed (nearly 14 min). Such long acquisition times can predispose to artifacts from patient motion. DTI VBA studies may be biased by differences in DTI data itself, including differences in data acquisition, processing, and analysis. Data processing, in particular, can have a large impact on study results. Although no parametric studies have been performed to understand all possible implications of processing parameters on data analysis, differences in smoothing (smoothing minimizes, to some degree, registration errors in VBA studies), for example, have been shown to produce different results depending on the filter size [29]. Finally, the VBA methodology suffers limitations related to errant subject-to-subject coregistration of images. Even healthy brains demonstrate moderate anatomical variability involving gray matter structures and, as a result, these variations affect the architecture of the intermediary white matter connections; however, VBA assumes anatomical conformity among subjects. TBSS has been proposed as an alternative to VBA as it eliminates result dependence on the degree of smoothing [30]. In combined studies with VBA and TBSS, the latter has generally shown to be more sensitive than VBA techniques [31, 32]. However, it is important to note that gold standard references for morphometric differences among clinical patient groups are generally lacking [33]. Additionally, size limitations for regions of differences detectable between two groups have been shown with TBSS, and the technique relies on skeletons to compare extremely variable white matter structures [34]. A study in this patient cohort was presented previously using TBSS analysis, and the results were generally concordant [35].

In summary, whole-brain VBA analysis reveals altered FA and RD in the optic chiasm and radiations of glaucoma patients. As FA and RD also correlate with glaucoma stage, these values could serve as potential noninvasive markers of disease severity.

Acknowledgments

This work was supported by the Natural Science Fund of China (81201079/81171393), a grant from the Shanghai Commission of Science and Technology #10440710200, and a grant from NIH/NIMH P50 MH090966-01.

References

1. Weinreb RN, Khaw PT. Primary open-angle glaucoma. Lancet. 2004; 363:1711–1720. [PubMed: 15158634]
2. Boland MV, Quigley HA. Risk factors and open-angle glaucoma: classification and application. J Glaucoma. 2007; 16:406–418. [PubMed: 17571004]
3. Gupta N, Yucel YH. Glaucoma as a neurodegenerative disease. Curr Opin Ophthalmol. 2007; 18:110–114. [PubMed: 17301611]
4. Dai H, Mu KT, Qi JP, Wang CY, Zhu WZ, Xia LM, Chen ZQ, Zhang H, Ai F, Morelli JN. Assessment of lateral geniculate nucleus atrophy with 3 T MR imaging and correlation with clinical stage of glaucoma. AJNR Am J Neuroradiol. 2011; 32:1347–1353. [PubMed: 21757515]
5. Kitsos G, Zikou AK, Bagli E, Kosta P, Argyropoulou MI. Conventional MRI and magnetisation transfer imaging of the brain and optic pathway in primary open-angle glaucoma. Br J Radiol. 2009; 82:896–900. [PubMed: 19433483]
6. Gupta N, Ang LC, de Tilly LN, Bidaisee L, Yucel YH. Human glaucoma and neural degeneration in intracranial optic nerve, lateral geniculate nucleus, and visual cortex. Br J Ophthalmol. 2006; 90:674–678. [PubMed: 16464969]
7. Gupta N, Yucel YH. What changes can we expect in the brain of glaucoma patients? Surv Ophthalmol. 2007; 52(Suppl 2):S122–126. [PubMed: 17998036]
8. Ito Y, Shimazawa M, Chen YN, Tsuruma K, Yamashima T, Araie M, Hara H. Morphological changes in the visual pathway induced by experimental glaucoma in Japanese monkeys. Exp Eye Res. 2009; 89:246–255. [PubMed: 19341728]
9. Yucel YH, Zhang Q, Weinreb RN, Kaufman PL, Gupta N. Effects of retinal ganglion cell loss on magno-, parvo-, koniocellular pathways in the lateral geniculate nucleus and visual cortex in glaucoma. Prog Retin Eye Res. 2003; 22:465–481. [PubMed: 12742392]
10. Qing G, Zhang S, Wang B, Wang N. Functional MRI signal changes in primary visual cortex corresponding to the central normal visual field of patients with primary open-angle glaucoma. Invest Ophthalmol Vis Sci. 2010; 51:4627–4634. [PubMed: 20357191]
11. Dai H, Morelli JN, Ai F, Yin D, Hu C, Xu D, Li Y. Resting-state functional MRI: functional connectivity analysis of the visual cortex in primary open-angle glaucoma patients. Hum Brain Mapp. 2012
12. Beaulieu C. The basis of anisotropic water diffusion in the nervous system—a technical review. NMR Biomed. 2002; 15:435–455. [PubMed: 12489094]
13. Augustinack JC, Helmer K, Huber KE, Kakunoori S, Zollei L, Fischl B. Direct visualization of the perforant pathway in the human brain with ex vivo diffusion tensor imaging. Front Hum Neurosci. 4:42. [PubMed: 20577631]
14. Tao XF, Wang ZQ, Gong WQ, Jiang QJ, Shi ZR. A new study on diffusion tensor imaging of the whole visual pathway fiber bundle and clinical application. Chin Med J (Engl). 2009; 122:178–182. [PubMed: 19187643]
15. Westlye LT, Walhovd KB, Dale AM, Bjornerud A, Due-Tonnessen P, Engvig A, Grydeland H, Tamnes CK, Ostby Y, Fjell AM. Life-span changes of the human brain white matter: diffusion tensor imaging (DTI) and volumetry. Cereb Cortex. 20:2055–2068. [PubMed: 20032062]
16. Song SK, Sun SW, Ramsbottom MJ, Chang C, Russell J, Cross AH. Dysmyelination revealed through MRI as increased radial (but unchanged axial) diffusion of water. NeuroImage. 2002; 17:1429–1436. [PubMed: 12414282]
17. Song SK, Sun SW, Ju WK, Lin SJ, Cross AH, Neufeld AH. Diffusion tensor imaging detects and differentiates axon and myelin degeneration in mouse optic nerve after retinal ischemia. NeuroImage. 2003; 20:1714–1722. [PubMed: 14642481]
18. Huang J, Friedland RP, Auchus AP. Diffusion tensor imaging of normal-appearing white matter in mild cognitive impairment and early Alzheimer disease: preliminary evidence of axonal degeneration in the temporal lobe. AJNR Am J Neuroradiol. 2007; 28:1943–1948. [PubMed: 17905894]

19. Bozzali M, Falini A, Franceschi M, Cercignani M, Zuffi M, Scotti G, Comi G, Filippi M. White matter damage in Alzheimer's disease assessed in vivo using diffusion tensor magnetic resonance imaging. J Neurol Neurosurg Psychiatr. 2002; 72:742–746. [PubMed: 12023417]
20. Naismith RT, Xu J, Tutlam NT, Trinkaus K, Cross AH, Song SK. Radial diffusivity in remote optic neuritis discriminates visual outcomes. Neurology. 2010; 74:1702–1710. [PubMed: 20498438]
21. Engelhorn T, Michelson G, Waerntges S, Struffert T, Haider S, Doerfler A. Diffusion tensor imaging detects rarefaction of optic radiation in glaucoma patients. Acad Radiol. 18:764–769. [PubMed: 21377906]
22. Garaci FG, Bolacchi F, Cerulli A, Melis M, Spano A, Cedrone C, Floris R, Simonetti G, Nucci C. Optic nerve and optic radiation neurodegeneration in patients with glaucoma: in vivo analysis with 3-T diffusion-tensor MR imaging. Radiology. 2009; 252:496–501. [PubMed: 19435941]
23. El-Rafei A, Engelhorn T, Warntges S, Dorfler A, Hornegger J, Michelson G. A framework for voxel-based morphometric analysis of the optic radiation using diffusion tensor imaging in glaucoma. Magn Reson Imaging. 2011; 29:1076–1087. [PubMed: 21802876]
24. Michelson G, Engelhorn T, Warntges S, El Rafei A, Hornegger J, Doerfler A. DTI parameters of axonal integrity and demyelination of the optic radiation correlate with glaucoma indices. Graefes Arch Clin Exp Ophthalmol. 2012
25. Zikou AK, Kitsos G, Tzarouchi LC, Astrakas L, Alexiou GA, Argyropoulou MI. Voxel-based morphometry and diffusion tensor imaging of the optic pathway in primary open-angle glaucoma: a preliminary study. AJNR Am J Neuroradiol.
26. Melonakos ED, Shenton ME, Rathi Y, Terry DP, Bouix S, Kubicki M. Voxel-based morphometry (VBM) studies in schizophrenia-can white matter changes be reliably detected with VBM? Psychiatry Res. 193:65–70. [PubMed: 21684124]
27. Smith SA, Williams ZR, Ratchford JN, Newsome SD, Farrell SK, Farrell JA, Gifford A, Miller NR, van Zijl PC, Calabresi PA, Reich DS. Diffusion tensor imaging of the optic nerve in multiple sclerosis: association with retinal damage and visual disability. AJNR Am J Neuroradiol. 2011; 32:1662–1668. [PubMed: 21799043]
28. Wheeler-Kingshott CA, Cercignani M. About "axial" and "radial" diffusivities. Magn Reson Med. 2009; 61:1255–1260. [PubMed: 19253405]
29. Jones DK, Symms MR, Cercignani M, Howard RJ. The effect of filter size on VBM analyses of DT-MRI data. NeuroImage. 2005; 26:546–554. [PubMed: 15907311]
30. Smith SM, Jenkinson M, Johansen-Berg H, Rueckert D, Nichols TE, Mackay CE, Watkins KE, Ciccarelli O, Cader MZ, Matthews PM, Behrens TE. Tract-based spatial statistics: voxelwise analysis of multi-subject diffusion data. NeuroImage. 2006; 31:1487–1505. [PubMed: 16624579]
31. Bodini B, Khaleeli Z, Cercignani M, Miller DH, Thompson AJ, Ciccarelli O. Exploring the relationship between white matter and gray matter damage in early primary progressive multiple sclerosis: an in vivo study with TBSS and VBM. Hum Brain Mapp. 2009; 30:2852–2861. [PubMed: 19172648]
32. Della Nave R, Ginestroni A, Tessa C, Salvatore E, Bartolomei I, Salvi F, Dotti MT, De Michele G, Piacentini S, Mascalchi M. Brain white matter tracts degeneration in Friedreich ataxia. An in vivo MRI study using tract-based spatial statistics and voxel-based morphometry. NeuroImage. 2008; 40:19–25. [PubMed: 18226551]
33. Haller S, Xekardaki A, Delaloye C, Canuto A, Lovblad KO, Gold G, Giannakopoulos P. Combined analysis of grey matter voxel-based morphometry and white matter tract-based spatial statistics in late-life bipolar disorder. J Psychiatry Neurosci. 2011; 36:391–401. [PubMed: 21284917]
34. Newlander, S. Methodological improvements in voxel based analysis of diffusion tensor images: aplications to study the impact of APOE on white matter integrity. San Diego State University; 2011. Dissertation
35. Dai, H.; Deng, X.; Li, Y.; Morelli, J.; Ai, F.; Guo, L.; Wang, C. Dorsal visual pathway neurodegeneration in patients with primary open angle glaucoma: in vivo analysis with 3 T diffusion-tensor MR imaging. 97th Scientific Assembly and Annual meeting of the Radiological Society of North America; Chicago, IL. 2011.

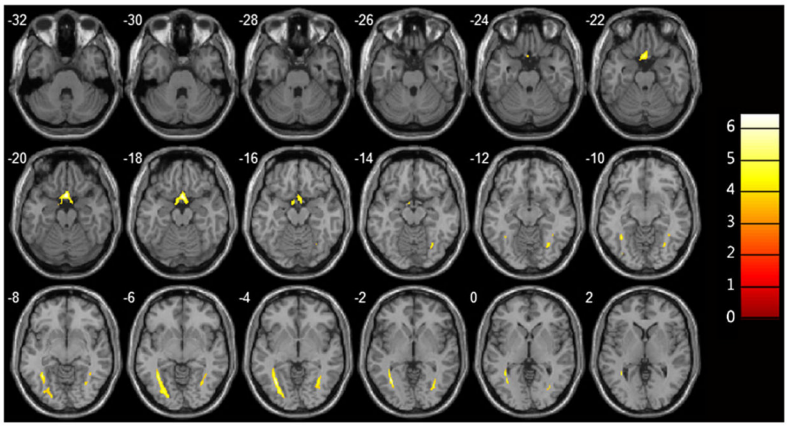

Fig. 1.

Overlay images demonstrating the statistically significant FA reductions in the optic chiasm and bilateral optic radiations of primary open angle glaucoma patients relative to those of healthy volunteers

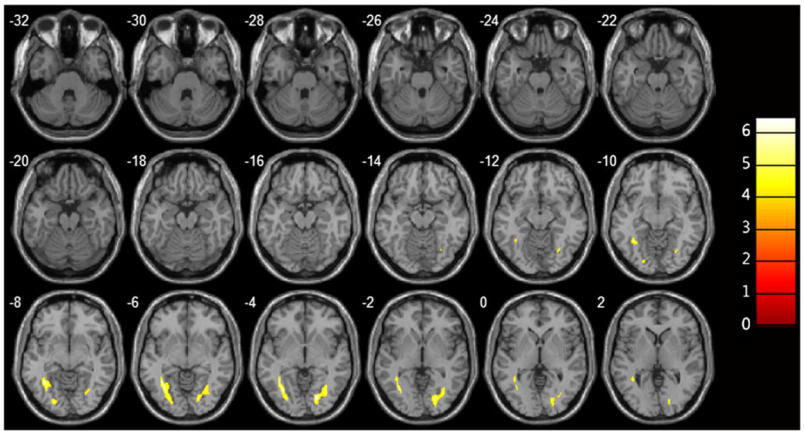

Fig. 2.

Overlay images demonstrating significantly greater RD in the optic radiations of glaucoma patients relative to those of healthy volunteers

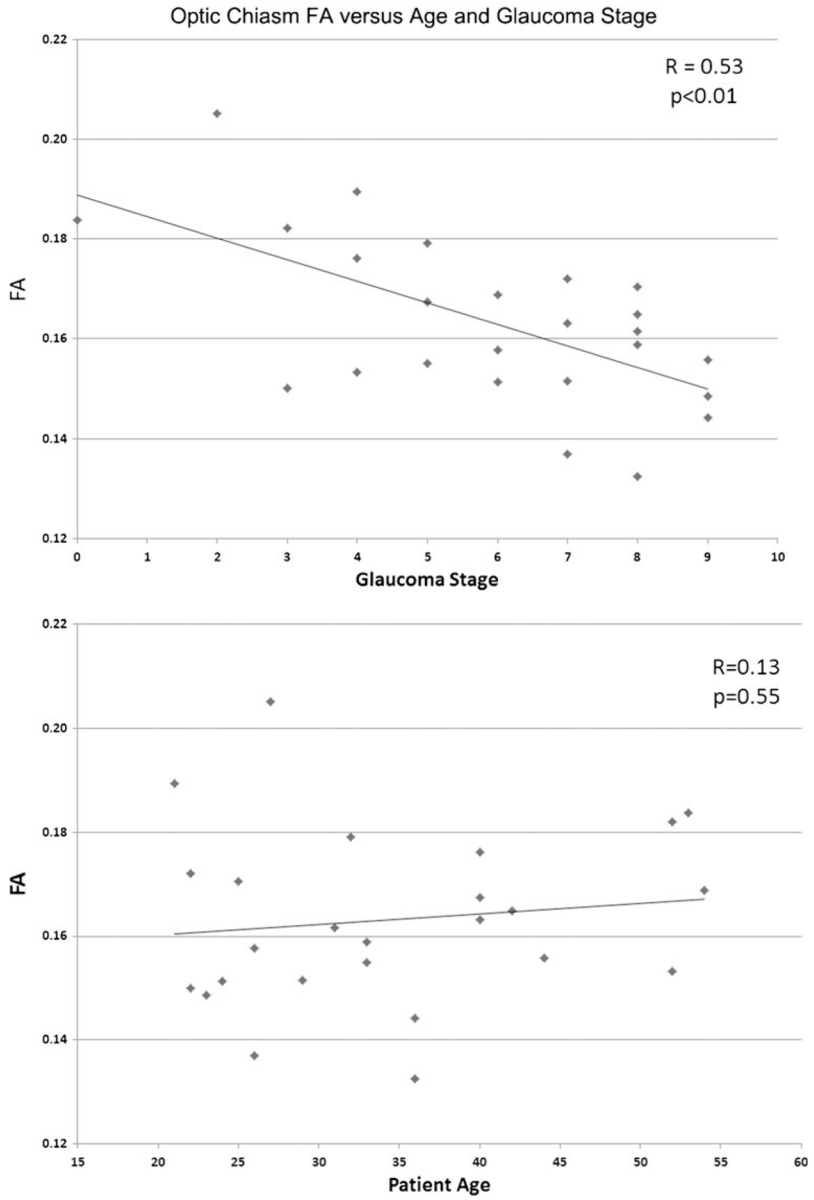

Fig. 3.

The FA values of the optic chiasm in patient group were negatively correlated with the sum of clinical stages of both eyes (r=0.53, p<0.01) but not statistically significantly correlated with patient age (r=0.13, p=0.55)

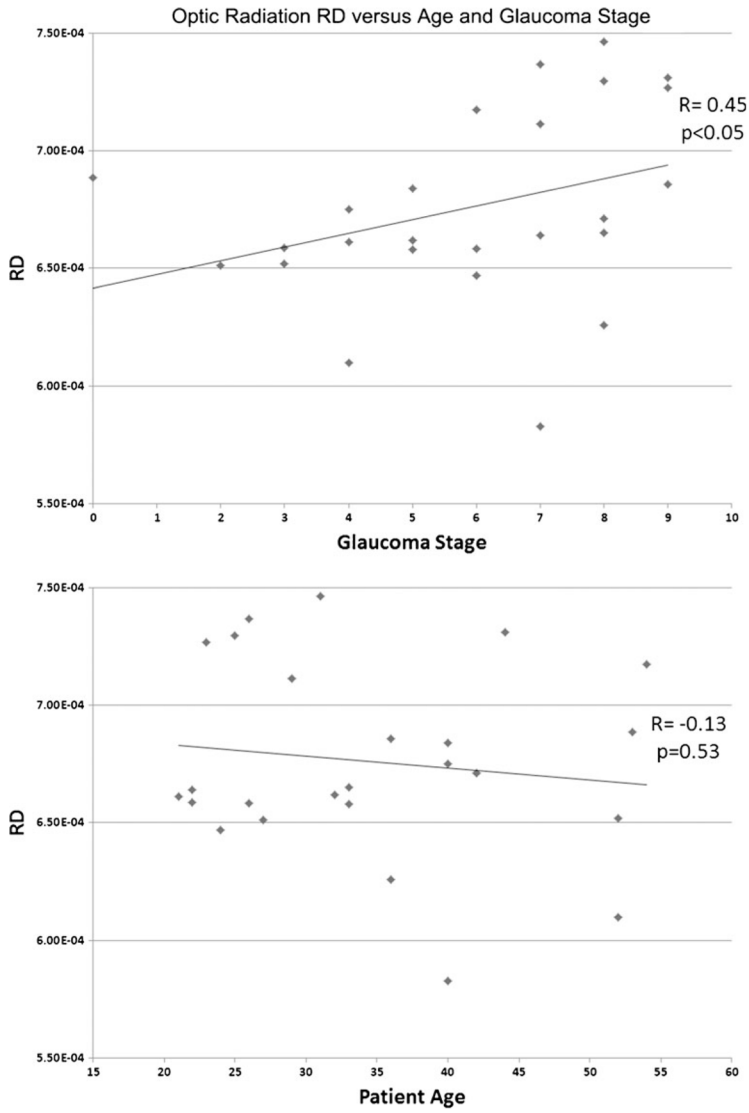

Fig. 4.

The RD values of the left optic radiation in the glaucoma group were positively correlated with the sum of clinical stages of both eyes (r=0.45, p<0.05) but not statistically significantly correlated with patient age (r=−0.13, p=0.53)

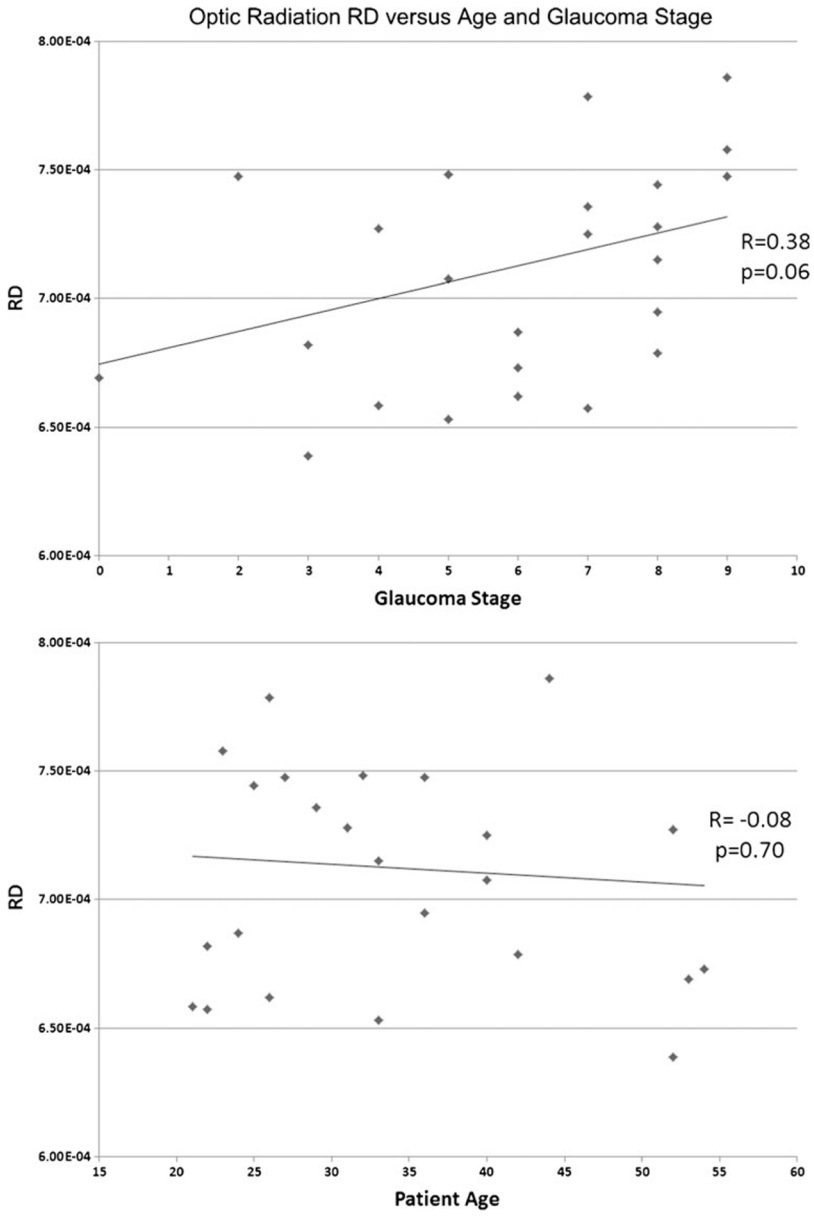

Fig. 5.

The RD values of the right optic radiation in the glaucoma group were positively correlated with the sum of clinical stages of both eyes, and a correlation just below the threshold of statistical significance was observed (r=0.38, p=0.06). No statistically significant correlation was seen with patient age (r=−0.08, p=0.70)

Table 1

The stage in HAP system and detailed data of ophthalmological examination of both eyes of 25 patients

	Stage-R	Stage-L	C/D-R	C/D-L	RNFL-R(um)	RNFL-L(um)	MDS-R	MDS-L
1	2	4	0.50	0.90	80.43	50.84	−10.40	−23.80
2	3	4	0.85	0.85	43.70	43.94	−18.50	−20.60
3	4	1	0.85	0.60	56.41	94.89	−22.30	−3.50
4	4	5	0.85	1.00	42.73	45.80	−21.90	Omit*
5	0	0	0.40	0.40	98.32	105.69	0.40	0.20
6	0	0	0.70	0.65	108.14	107.28	0.30	0.50
7	3	3	0.80	0.85	71.44	41.99	−13.20	−17.50
8	1	4	0.65	0.95	104.26	73.96	−1.40	−21.20
9	3	2	0.85	0.8	58.60	82.25	−12.70	−8.50
10	4	4	0.90	0.95	47.79	42.05	−24.40	−21.10
11	5	2	0.95	0.90	41.21	54.35	Omit*	−11.70
12	5	3	0.90	0.80	36.43	55.63	Omit*	−16.20
13	3	1	0.75	0.50	54.95	72.10	−17.70	−1.90
14	0	4	0.45	0.90	88.64	55.44	0.80	−23.90
15	4	3	0.90	0.90	50.21	56.45	−21.40	−13.80
16	4	0	0.90	0.40	39.74	95.76	−24.60	0.10
17	5	4	1.00	0.90	42.16	53.53	Omit*	−22.30
18	4	5	0.90	1.00	46.86	39.30	−24.60	Omit*
19	2	1	0.60	0.50	58.91	88.21	−2.10	−13.60
20	2	4	0.60	0.75	78.96	60.14	−9.80	−24.40
21	4	4	0.85	0.80	58.76	55.92	−20.30	−20.90
22	2	1	0.90	0.80	63.55	83.5	−7.80	−4.50
23	2	5	0.85	1.00	40.80	69.49	−8.60	Omit*
24	4	4	0.90	0.90	35.52	36.61	−20.20	−21.40
25	4	4	0.90	0.90	43.13	55.13	−22.90	−21.60

Omit* means eye in stage 5 without MD value detected *C/D* cup to disk ratio, *RNFL* retinal nerve fiber layer thickness, *MD* mean deviation score, *R* right, *L* left

Table 2

Brain regions with significant differences of FA between control and POAG group ($p<0.05$)

Brain region	BA	Cluster size (mm^3)	MNI axis			T value
			X	Y	Z	
Optic chiasm		690	1.18	13.12	−20	7.035
Right optic radiation		407	33.14	−63.02	−4	4.9475
Left optic radiation		1065	−32.66	−62.08	−4	6.6317

BA Brodmann area

Table 3

Brain regions with significant differences of RD between control and POAG group ($p<0.05$)

Brain region	BA	Cluster size (mm^3)	MNI axis			T value
			X	Y	Z	
Right optic radiation		987	19.98	−76.18	−4	−6.2546
Left optic radiation		1176	−36.42	−53.62	−8	−6.4235

BA Brodmann area

Table 4

Correlation coefficients between areas of DTI parameter changes in glaucoma patients and mean retinal nerve thickness

	Mean retinal nerve thickness (mm)	
	R	***p* value**
Optic Chiasm FA	0.63	<0.001
Left Radiation FA	0.20	0.3
Right Radiation FA	0.31	0.1
Left Radiation RD	−0.26	0.2
Right Radiation RD	−0.30	0.1